1 Supernova Sample and Notes for Individual SNe

Supplementary Table 1 summarizes the data of the SNe used in the present study. The values of the velocity gradients ($\dot{v}_{\rm Si}$) are obtained from the literature when available. They are mostly drawn from a previous compilation[10] (see Supplementary Tab. 1 for the sources of the observations), with values for additional SNe obtained from the references listed in Supplementary Table 1. For SN 1998aq, we have measured $\dot{v}_{\rm Si}$ from the published spectra[38].

The line-of-sight velocity of the deflagration ash is derived as follows. Late-time spectra of SNe Ia show various forbidden lines from Fe-peak elements. These lines can be divided into two groups. The first group requires intense heating from radioactive ^{56}Ni $\rightarrow$ ^{56}Co $\rightarrow$ ^{56}Fe decays and low material density (e.g., [Fe III] λ4701), while the second group requires a low heating rate and high material density (e.g., [Fe II] λ7155 and [Ni II] λ7378). Considering general properties of the emission process[19], the former lines are argued to be preferentially emitted from the detonation ash (because it is at relatively low density with a large amount of ^{56}Ni), while the latter lines are formed in the deflagration ash (because it is at high density with a small amount of ^{56}Ni). These two groups of lines show mutually different properties in observations, strengthening the interpretation that they are emitted from different regions: The 'deflagration ash'-lines show the diversity in Doppler shift (not only in [Fe II] λ7155 and [Ni II] λ7378[61,62]), while the 'detonation ash'-lines show virtually no Doppler shifts. This property led to the conclusion that the deflagration ash is on

average located offset, while the detonation ash is distributed roughly spherically[19].

For $v_{\rm neb}$ (the line-of-sight velocity of the deflagration ash), we have therefore measured the wavelength shift in [Ni II] λ7378 and in [Fe II] λ7155, and defined $v_{\rm neb}$ as the mean value of them (see Supplementary Tab. 1 for the source of the observational data). The error bars are taken to be the difference in the measurements for the two lines. In all SNe except for SN 2004dt, the difference in these two measurements is at most 600 km s^{-1}. For SNe Ia in which either of [Fe II] λ7155 or [Ni II] λ7378 is weak and unidentified, we measure $v_{\rm neb}$ only from the other single line, with a conservative error of 600 km s^{-1}. For SNe 2007on, 2007sr, and 2009ab, we have measured $\dot{v}_{\rm Si}$ and $v_{\rm neb}$ from our own spectra taken at the Gemini South, the Magellan, and the ESO (La Silla, Paranal) telescopes. The late-time spectrum of SNe 1997bp has also been obtained by us and used to measure $v_{\rm neb}$. The 20 SNe in Supplementary Table 1 are all the objects we have found for which both $\dot{v}_{\rm Si}$ and $v_{\rm neb}$ are reliably available to date. Also shown in the table are the light-curve decline-rate parameters $\Delta m_{15}(B)$.

Supplementary Table 1 also lists the epoch (after B-band maximum) of the late-time spectra from which $v_{\rm neb}$ is measured. For most of the SNe Ia, it is at least 200 days after B-band maximum, and thus errors caused by the blending of additional lines to this feature (e.g., permitted lines emitted at relatively early phases) in measuring $v_{\rm neb}$ can be avoided. The features at $\sim 7,000 - 7,500$ Å, which we interpret to be dominated by [Fe II] λ7155 and [Ni II] λ7378, do not show significant evolution at $\gtrsim 100 - 150$ days after B-band maximum[19].

It has been shown that normal SNe Ia[18] (which constitute $\gtrsim 80$% of the whole SN Ia popu-

lation), faint 1991-bg like SNe Ia[26], and bright 1991T-like SNe Ia[63,64] show different properties in $\dot{v}_{\rm Si}$[10]. Normal SNe Ia show a diversity in $\dot{v}_{\rm Si}$, which is apparently *not* correlated with $\Delta m_{15}(B)$. Faint 1991bg-like SNe Ia, which are characterized by a rapid fading (i.e., large $\Delta m_{15}(B)$), always show large $\dot{v}_{\rm Si}$. Bright 1991T-like SNe Ia with small $\Delta m_{15}(B)$ always show small $\dot{v}_{\rm Si}$. In deriving $v_{\rm neb}$, we have noticed that the identification of [Fe II] λ7155 and [Ni II] λ7378 is robust for normal SNe Ia, but tends to be a subject of possible misidentification for the other subclasses (then such SNe Ia are omitted from our analysis): Faint 1991bg-like SNe Ia tend to show probable [Ca II] λ7291, 7324 [27]. Bright 1991T-like SNe Ia tend to show a broad single peak, possibly indicating that [Fe II] λ7155 and [Ni II] λ7378 are broad and mutually blended. These indicate that the ejecta structure (density, temperature, and composition) of faint and bright SNe Ia is intrinsically different from normal ones. This is a reason why our sample is mainly composed of normal SNe Ia. Luckily, omitting a large fraction of faint/bright SNe Ia is not important for our present analysis, since we are interested in the spectral diversity beyond the one-parameter $\Delta m_{15}(B)$ description, which is a problem only in normal SNe Ia.

For normal SNe Ia, we categorize HVG SNe and LVG SNe according to $\dot{v}_{\rm Si}$, with the division line at 70 km s^{-1} day^{-1}. According to its $\dot{v}_{\rm Si}$, SN 2004dt is an HVG. However, its peculiar observational features suggest that it is an outlier, and the origins of its high velocity gradient and the negative $v_{\rm neb}$ are likely different than the one for other HVGs (see Fig. 2 caption). One of the peculiar features of SN 2004dt appears in its late-time spectra. Supplementary Fig. 1 shows a late-time spectrum of SN 2004dt compared to the prototypical faint SN 1991bg and to the normal HVG SN 2007sr. The spectrum of SN 2004dt provides a good match to that of the faint SN 1991bg. Both

the intensity and the width of the lines at $\sim 7,000 - 7,500$ Å are similar for these two SNe. In normal HVG SN 2007sr, the features at $7,000 - 7,500$ Å are much fainter than for SNe 2004dt and 1991bg. This indicates that in the case of SN 2004dt the feature is probably contaminated by other lines, most likely [Ca II] $\lambda\lambda$7291, 7324 (note that SN 2004dt shows a larger error in $v_{\rm neb}$ than the other SNe Ia). In addition, the strongest lines at late phases, i.e., the [Fe III] blend at $\sim 4,700$ Å and the [Fe II] and [Fe III] blend at $\sim 5,250$ Å have similar ratios in SN 2004dt and 1991bg; these ratios have been noticed to be peculiar[29]. The normal HVG SN 2007sr has broader lines, and different line ratios. These similarities between the 'normal' SN 2004dt and the faint SN 1991bg at late phases, which have not been noticed previously, suggest that these explosions might be closely related to one another. SN 2004dt may represent a new class of SNe Ia[65] which have SN 1991bg-like features in the late-time spectrum, but are more energetic and brighter.

Supplementary Table 1: Supernovae Sample

SN	$\Delta m_{15}(B)$	$\dot{v}_{\rm Si}$ (km s^{-1} day^{-1})	$v_{\rm neb}$ (km s^{-1})	Epoch (day)	Class[8,24]	References
1986G	1.81 ± 0.07	64 ± 5	-680 ± 50	257	HVG/Faint	1, 31, 32
1990N	1.07 ± 0.05	41 ± 5	-1130 ± 600	280	LVG	1, 10, 33, 34
1994D	1.32 ± 0.05	39 ± 5	-1440 ± 390	306	LVG	1, 34, 35
1997bp	0.97 ± 0.2	106 ± 7	2650 ± 150	300	HVG	10, 36
1998aq	1.12 ± 0.05	35 ± 4	-1100 ± 50	241	LVG	37, 38
1998bu	1.06 ± 0.05	10 ± 5	-990 ± 150	329	LVG	1, 10, 24, 25, 39
2000cx	0.93 ± 0.04	2 ± 4	-320 ± 600	147	LVG/peculiar	40-43
2001el	1.13 ± 0.04	31 ± 5	1070 ± 230	398	LVG	44-46
2002bo	1.16 ± 0.06	110 ± 7	1900 ± 220	368	HVG	17, 21
2002dj	1.08 ± 0.05	86 ± 6	2100 ± 420	275	HVG	47
2002er	1.32 ± 0.03	92 ± 5	890 ± 600	216	HVG	48, 49
2003du	1.02 ± 0.05	31 ± 5	-370 ± 50	377	LVG	50, 51
2003hv	1.61 ± 0.02	41 ± 6	-2750 ± 440	320	LVG	52
2004dt	1.21 ± 0.05	160 ± 15	-1910 ± 1070	152	HVG/peculiar	29
2004eo	1.45 ± 0.04	45 ± 4	0 ± 600	228	LVG	53, 54
2005cf	1.12 ± 0.03	35 ± 5	420 ± 600	267	LVG	55-58
2006X	1.31 ± 0.05	123 ± 10	1280 ± 20	277	HVG	59
2007on	1.62 ± 0.01	85 ± 6	0 ± 600	356	HVG/Faint	This work
2007sr	0.93 ± 0.02	80 ± 15	1910 ± 400	256	HVG	60
2009ab	1.20 ± 0.02	36 ± 13	-410 ± 410	278	LVG	This work

2 Other Observational Constraints

In abundance 'tomography'[16,21,66−68], a temporal sequence of spectra of individual SNe Ia are used to infer the distribution of different elements through the SN ejecta, assuming the density structure of a spherically symmetric explosion model[13]. From this type of analysis, it has been indicated that the abundance distribution is generally a function of $\Delta m_{15}(B)$. The difference between the HVG and LVG SNe, not related to $\Delta m_{15}(B)$, is mainly on the extent of the Si-rich layer[16] and on the photospheric velocity[66], which are explained by our proposed scenario (main text).

On the other hand, the spatial extent of the ^{56}Ni-rich region does not seem to be dependent on whether it is a HVG or a LVG SN[16]. This could provide a constraint on the ejecta asymmetry. In the offset explosion model, the spatial extent of the ^{56}Ni region, as well as the density structure at the outer edge of that region, are not sensitive to the direction, despite the initially large asymmetry in the ignition[6]. This stems from the nature of the propagation of the detonation wave as described in the main text; unlike the deflagration flame, the detonation tries to expand isotropically, producing roughly spherically distributed ^{56}Ni. This region is not sensitively affected by the existence of the deflagration ashes, which is essential in determining the structure of Si-rich region. As a result, the spatial extent of the ^{56}Ni-rich region is mainly controlled by the different amounts of ^{56}Ni produced in the explosion, and the viewing angle dependence could add some diversity at most as a secondary effect[6]; this is consistent with the observational indications[16].

The asymmetric distribution of the outermost layer may imprint its signature in polarization measurements, which may be linked to the velocity gradient[69]. The polarization of the Si II line

is correlated with $\Delta m_{15}(B)$[22], but only for LVG SNe (Supplementary Fig. 2). HVG SNe generally show larger polarization than LVG SNe[70,71] but they clearly do not follow this trend. A global one-sided asymmetry as in the present interpretation would produce relatively low continuum polarization and relatively high line polarization at Si II λ6355[72]. In our proposed scenario the global asymmetry is of smaller degree than in an extremely asymmetric model producing Si II polarization of $\sim 1\%$[72], thus this is likely not a major contributor to the observed polarization. Alternatively, it has been suggested, based on the correlation between the Si II polarization and $\Delta m_{15}(B)$, that the observed Si II polarization could be a measure of the thickness of the outer layer above the ^{56}Ni-rich region, in which the local inhomogeneity, e.g., a few relatively dense blobs, is assumed to be a source of polarization. In this interpretation, the large Si II polarization in HVG SNe could be a consequence of an extended outer layer in the direction opposite to the initial sparks.

3 Viewing-Angle Effect on the Light Curve

It has been suggested that if the ejecta are asymmetric, $\Delta m_{15}(B)$ is dependent on the direction to the observer[5]. Supplementary Fig. 3 shows the comparison between $\Delta m_{15}(B)$ and $v_{\rm neb}$ for SNe Ia.

In the same figure, the possible effect of the viewing angle on the light curve shape, and the implication on the scatter in the luminosity calibration beyond the one-parameter description, are schematically illustrated. For example, the LVG SN 1998bu and the HVG SN 2002bo had similar $\Delta m_{15}(B)$ values, and this could be interpreted as follows.

These two SNe would indeed have intrinsically different amounts of $M(^{56}\mathrm{Ni})$ and accordingly different luminosity. Because of different $M(^{56}\mathrm{Ni})$, $\Delta m_{15}(B)$ would be different if viewed from the same direction. Assuming that (1) $\Delta m_{15}(B)$ would be smaller and the luminosity is thus larger for LVG SN 1998bu than for HVG SN 2002bo, for a putative observer at the same direction, and that (2) $\Delta m_{15}(B)$ appears larger for an observer closer to the offset direction, as a viewing angle effect. Then, these two SNe would show similar $\Delta m_{15}(B)$ as observed, despite the intrinsic difference in luminosity, since the viewing direction is closer to the offset direction for SN 1998bu.

This effect would produce a scatter in the luminosity of SNe Ia, around the standard luminosity determined by $M(^{56}\mathrm{Ni})$. Pairs of SNe with similar $\Delta m_{15}(B)$, as a result of the viewing angle originating from SNe with different amounts of $M(^{56}\mathrm{Ni})$, are naturally expected if we observe a large number of SNe Ia (Sup. Fig. 3) for the following two reasons: (1) SNe Ia do indeed show large variations in $M(^{56}\mathrm{Ni})$, and (2) the viewing angles should display large variations.

A question for this interpretation is whether any indication of such an effect is seen in the data. Supplementary Fig. 3 shows that there is no clear (but perhaps a marginal) correlation between $\Delta m_{15}(B)$ and $v_{\rm neb}$. According to the prediction[5] of the viewing-angle effect on $\Delta m_{15}(B)$ for models similar to the one shown in the main text, the observed $\Delta m_{15}(B)$ could vary by ~ 0.4 mag depending on the direction to the observer (schematically shown in Sup. Fig. 3). This is smaller than the intrinsic variation in $\Delta m_{15}(B)$ for different $M(^{56}\mathrm{Ni})$, and thus such an effect is difficult to notice in Supplementary Fig. 3, as is consistent with the low correlation in the present data. Any marginal correlation between $\Delta m_{15}(B)$ and $v_{\rm neb}$ may already hint that such an effect is indeed there, but a larger number of SNe Ia is necessary to test this possibility with statistical significance.

4 Supplementary Figure 1

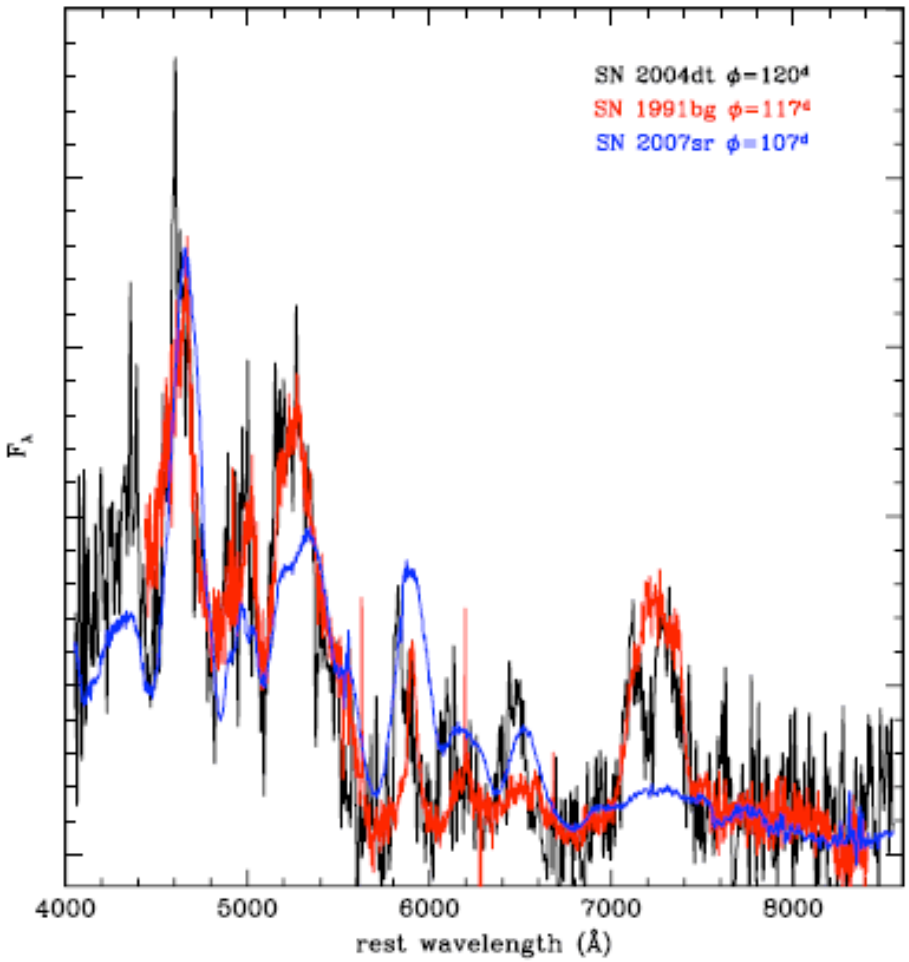

Spectrum of SN 2004dt[29] at 120 days after B-band maximum, compared to those of the faint SN 1991bg[27] and of the normal HVG SN 2007sr at similar epochs.

5 Supplementary Figure 2

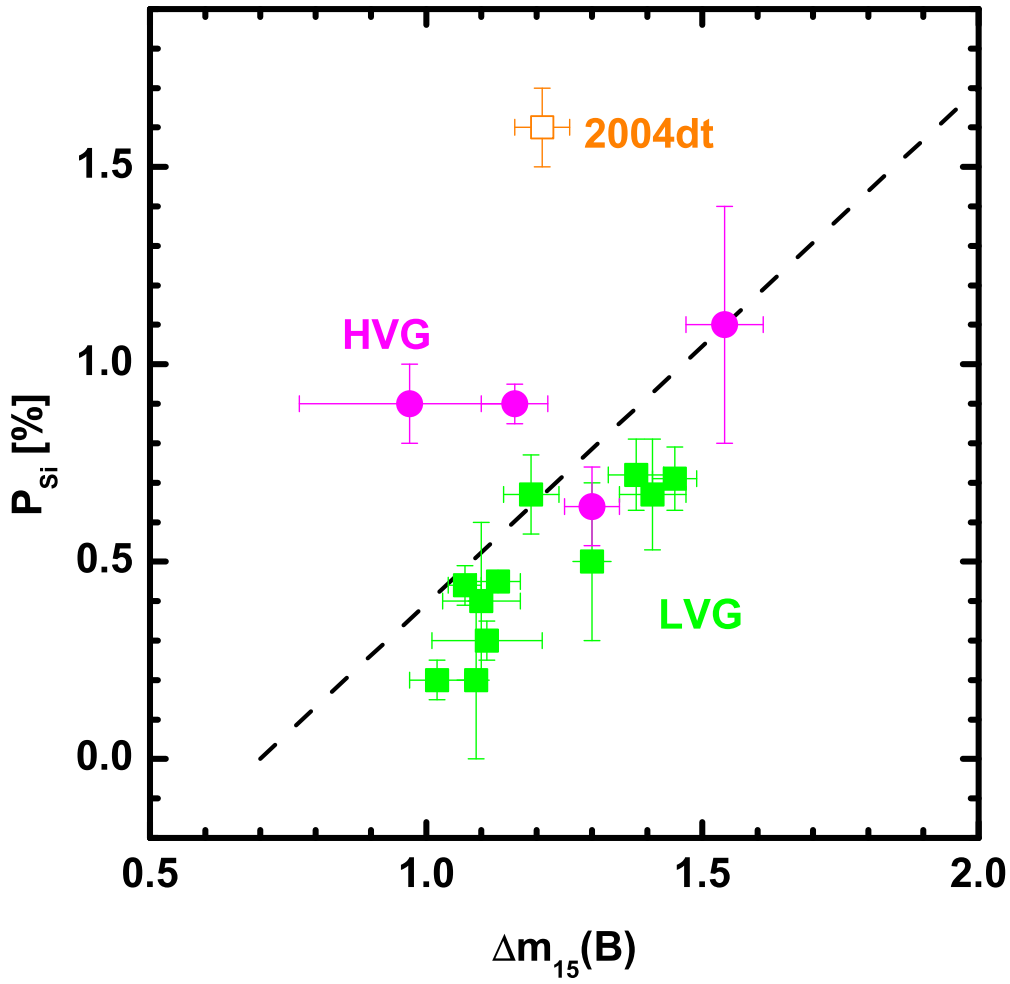

Si II λ6355 line polarization for SNe Ia, as a function of the decline-rate parameter[22,70,71]. The dashed line shows a linear fit to the data excluding SN 2004dt[22]. The colors of the symbols are the same as in Fig. 2 of the main text.

6 Supplementary Figure 3

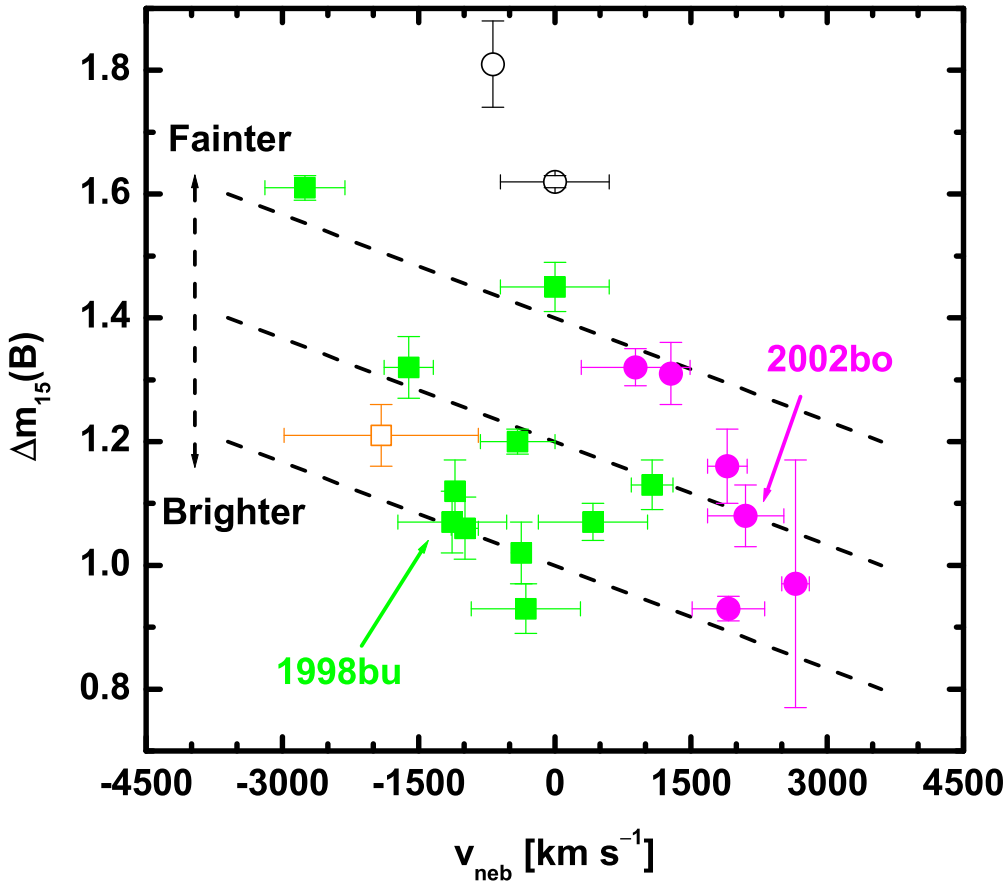

The decline-rate parameter $\Delta m_{15}(B)$ versus the late-time emission-line velocity shift. The three dashed lines schematically illustrate the expected viewing angle effect on the decline-rate parameter, which would produce a ~ 0.4 mag difference in the observed $\Delta m_{15}(B)$ for an observer in the offset direction as opposed to the opposite direction[5]. The lines correspond to three hypothesized explosion configurations which are mutually different in $M(^{56}\mathrm{Ni})$ and therefore in the intrinsic luminosity.

31. Phillips, M. M., et al., The Type Ia Supernova 1986G in NGC 5128 - Optical Photometry and Spectra, Pub. Astron. Soc. Pac., **99**, 592-605 (1987)

32. Cristiani, S., et al., The SN 1986 G in Centaurus A, Astron. Astrophys., **259**, 63-70 (1992)

33. Leibundgut, B., et al., Premaximum Observations of the Type Ia SN 1990N, Astrophys. J., **371**, L23-L26 (1991)

34. Gómez, G., López, R., Sánchez, F., The Canaris Type Ia Supernovae Archive (I), Astron. J., **112**, 2094-2109 (1996)

35. Patat, F., et al., The Type Ia Supernova 1994D in NGC 4526: The Early Phases, Mon. Not. R. Astron. Soc., **278**, 111-124 (1996)

36. Altavilla, G., et al., Cepheid Calibration of Type Ia Supernovae and The Hubble Constant, Mon. Not. R. Astron. Soc., **349**, 1344-1352 (2004)

37. Riess, A. G., et al., The Rise Time of Nearby Type Ia Supernovae, Astron. J., **118**, 2675-2688 (1999)

38. Branch, D., et al., Optical Spectra of The Type Ia Supernova 1998aq, Astron. J., **126**, 1489-1498 (2003)

39. Hernandez, M., et al., An Early-Time Infrared and Optical Study of The Type Ia Supernova 1998bu in M96, Mon. Not. R. Astron. Soc., **319**, 223-234 (2000)

40. Li, W., et al., The Unique Type Ia Supernova 2000cx in NGC 524, Pub. Astron. Soc. Pac., **113**, 1178-1204 (2001)

41. Patat, F., et al., Upper Limit for Circumstellar Gas around The Type Ia SN 2000cx, Astron. Astrophys., **474**, 931-936 (2007)

42. Candia, P., et al., Optical and Infrared Photometry of the Unusual Type Ia Supernova 2000cx, Pub. Astron. Soc. Pac., **115**, 277-294 (2003)

43. Sollerman, J., et al., The Late-Time Light Curve of The Type Ia Supernova 2000cx, Astron. Astrophys., **428**, 555-568 (2004)

44. Krisciunas, K., et al., Optical and Infrared Photometry of the Nearby Type Ia Supernova 2001el, Astron. J., **125**, 166-180 (2003)

45. Wang, L., et al., Spectropolarimetry of SN 2001el in NGC 1448: Asphericity of a Normal Type Ia Supernova, Astrophys. J., **591**, 1110-1128 (2003)

46. Mattila, S., et al., Early and Late Time VLT Spectroscopy of SN 2001el - Progenitor Constraints for a Type Ia Supernova, Astron. Astrophys., **443**, 649-662 (2005)

47. Pignata, G., et al., Optical and Infrared Observations of SN 2002dj: Some Possible Common Properties of Fast-Expanding Type Ia Supernovae, Mon. Not. R. Astron. Soc., **388**, 971-990 (2008)

48. Pignata, G., et al., Photometric Observations of The Type Ia SN 2002er in UGC 10743, Mon. Not. R. Astron. Soc., **355**, 178-190 (2004)

49. Kotak, R., et al., Spectroscopy of The Type Ia Supernova SN 2002er: Days -11 to +215, Astron. Astrophys., **436**, 1021-1031 (2005)

50. Anupama, G. C., Sahu, D. K., Jose, J., Type Ia Supernova SN 2003du: Optical Observations, Astron. Astrophys., **429**, 667-676 (2005)

51. Stanishev, V., et al., SN 2003du: 480 days in The Life of a Normal Type Ia Supernova, Astron. Astrophys., **469**, 645-661 (2007)

52. Leloudas, G., et al., The Normal Type Ia SN 2003hv out to Very Late Phases, Astron. Astrophys., **505**, 265-279 (2009)

53. Pastorello, A., ESC and KAIT Observations of The Transitional Type Ia SN 2004eo, Mon. Not. R. Astron. Soc., **377**, 1531-1552 (2007)

54. Hachinger, S., Mazzali, P.A., & Benetti, S., Exploring the Spectroscopic Diversity of Type Ia Supernovae, Mon. Not. R. Astron. Soc., **370**, 299-318 (2006)

55. Pastorello, A., et al., ESC Observations of SN 2005cf - I. Photometric Evolution of a Normal Type Ia Supernova, Mon. Not. R. Astron. Soc., **376**, 1301-1316 (2007)

56. Wang, X., et al., The Golden Standard Type Ia Supernova 2005cf: Observations from The Ultraviolet to The Near-Infrared Wavebands, Astrophys. J., **697**, 380-408 (2009)

57. Leonard, D. C., Constraining the Type Ia Supernova Progenitor: The Search for Hydrogen in Nebular Spectra, AIP Conference Proceedings, **937**, 311-315 (2007)

58. Garavini, G., et al., ESC Observations of SN 2005cf. II. Optical Spectroscopy and The High-Velocity Features, Astron. Astrophys., **471**, 527-535 (2007)

59. Wang, X. et al., Optical and Near-Infrared Observations of the Highly Reddened, Rapidly Expanding Type Ia Supernova SN 2006X in M100, Astrophys. J., **675**, 626-643 (2008)

60. Schweizer, F., et al., A New Distance to the Antennae Galaxies (NGC 4038/39) Based on The Type Ia Supernova 2007sr, Astron. J., **136**, 1482-1489 (2008)

61. Motohara, K., et al., The Asymmetric Explosion of Type Ia Supernovae as Seen from Near-Infrared Observations, Astrophys. J., **652**, L101-L104 (2006)

62. Gerardy, C.L., et al., Signatures of Delayed Detonation, Asymmetry, and Electron Capture in

the Mid-Infrared Spectra of Supernovae 2003hv and 2005df, Astrophys. J., **661**, 995-1012 (2007)

63. Filippenko, A.V., et al., The peculiar Type Ia SN 1991T - Detonation of a white dwarf?, Astrophys. J., **384**, L15-L18 (1992)

64. Phillips, M. M., et al., SN 1991T - Further evidence of the heterogeneous nature of type Ia supernovae, Astron. J., **103**, 1632-1637 (1992)

65. Pakmor, R., et al., Sub-Luminous Type Ia Supernovae from The Mergers of Equal-Mass White Dwarfs with Mass $\sim 0.9M_{\odot}$, Nature, **463**, 61-64 (2010)

66. Tanaka, M., et al., The Outermost Ejecta of Type Ia Supernovae, Astrophys. J., **677**, 448-460 (2008)

67. Mazzali, P.A., Sauer, D.N., Pastorello, A., Benetti, S., & Hillebrandt, W., Abundance Stratification in Type Ia Supernovae - II. The Rapidly Declining, Spectroscopically Normal SN 2004eo, Mon. Not. R. Astron. Soc., **386**, 1897-1906 (2008)

68. Hachinger, S., Mazzali, P. A., Taubenberger, S., Pakmor, R., & Hillebrandt, W., Spectral Analysis of The 91bg-like Type Ia SN 2005bl: Low Luminosity, Low Velocities, Incomplete Burning, Mon. Not. R. Astron. Soc., **399**, 1238-1254 (2009)

69. Patat, F., Baade, D., Höflich, P., Maund, J. R., Wang, L., Wheeler, J. C., VLT Spectropolarimetry of The Fast Expanding Type Ia SN 2006X, Astron. Astrophys., **508**, 229-246 (2009)

70. Leonard, D.C., Li, W., Filippenko, A.V., Foley, R.J., & Chornock, R., Evidence for Spectropolarimetric Diversity in Type Ia Supernovae, Astrophys. J., **632**, 450-475 (2005)

71. Chornock, R., & Filippenko, A.V., Deviation from Axisymmetry Revealed by Line Polarization in the Normal Type Ia Supernova 2004S, Astron. J., **136**, 2227-2237 (2008)

72. Kasen, D., & Plewa, T., Detonating Failed Deflagration Model of Thermonuclear Supernovae.

II. Comparison to Observations, Astrophys. J., **662**, 459-471 (2007)